CONEM 2010 VI Congresso Nacional de Engenharia Mecânica

ABCM COMPROMETIDA COM A PROMOÇÃO DO DESENVOLVIMENTO DA ENGENHARIA E DAS CIÊNCIAS MECÂNICAS
ASSOCIAÇÃO BRASILEIRA DE ENGENHARIA E CIÊNCIAS MECÂNICAS

VI CONGRESSO NACIONAL DE ENGENHARIA MECÂNICA
VI NATIONAL CONGRESS OF MECHANICAL ENGINEERING
18 a 21 de agosto de 2010 – Campina Grande – Paraíba - Brasil
August 18 – 21, 2010 – Campina Grande – Paraíba – Brazil

H_2 OPTIMAL CONTROL FOR EARTHQUAKE EXCITED STRUCTURES

Gustavo Luiz C. M. Abreu, gustavo@dem.feis.unesp.br[1]
Vicente Lopes Jr., vicente@dem.feis.unesp.br[1]

[1] Grupo de Materiais e Sistemas Inteligentes – GMSINT, Faculdade de Engenharia de Ilha Solteira - FEIS, Departamento de Engenharia Mecânica, Av. Brasil, 56, Ilha Solteira-SP, Brasil, Zip Code: 15385000.

Abstract. *This paper investigates a systematic procedure on applying H_2 optimal control algorithm for controlling the lateral vibration of earthquake excited structures. Based on a dynamic model of the structural system, the filter on an earthquake input model, sensor noise and control output are incorporated into the plant to produce an H_2 optimal controller based on acceleration feedback. The performance of the controller in reducing the response of seismically excited structure is tested experimentally in a two-story building test-bed subjected to earthquake ground acceleration using a shaking table system and controlled by an active mass driver.*

Keywords: *Active Vibration Control, H_2 Optimal Control, Building Model, Active Mass Driver.*

1. INTRODUCTION

The control of structural vibration has significant increase in the last two decades. One of the application areas for control design has to do with the protection of civil engineering structures from dynamic loadings such as high wind and strong earthquakes (Housner et al., 1997). In the last 15 years, world-wide attention has been directed toward the use of control to mitigate the effects of these dynamic loads. Spencer and Sain (1997) reviewed the state-of-the art in structural vibration control for civil engineering applications. Among those studies, different kinds of control devices and control algorithms were presented.

Optimal control design methods which are carried out in the frequency domain have recently been applied in control of civil structures and offer attractive features. It is well known that the dynamic behavior of structures, as well as the excitations, is often characterized by functions in the frequency domain (Spencer et al., 1994). The transfer function of a structure in the frequency domain can be obtained directly from modal tests, and random signals such as earthquake and wind loads can be modeled by a spectral density function. Frequency domain optimal control strategies allow the designer to directly deal with these natural representations of the structural model and excitation during control design. These methods also allow the designer to specify disturbance attenuation over a desired frequency range, as well as to roll-off the control action at high frequencies where measurement noise and uncertainties may plague the controlled structure. In the frequency domain, the desired controller can be achieved by a proper selection of frequency-dependent weighting functions and filters modeling earthquake disturbances.

Two frequency domain methods for controller design which have received much attention recently are: H_2 and H_∞ control strategies (Doyle et al., 1989). The H_2 and the H_∞ control methods give optimal controllers by minimizing, respectively, the H_2 and the H_∞ norms of the transfer function from the input excitation to the structural responses. Suhardjo et al (1992) provided a numerical comparison between the H_2 and H_∞ approaches to active control of wind-excited buildings. Spencer et al. (1994) was the first to apply H_2 control strategy to civil engineering structures for seismic protection purposes. Dyke et al. (1996) developed a mathematical model for a scaled building structure through system identification in the frequency domain. In that paper, a H_2 controller was designed using dynamic feedback of acceleration responses and its performance was verified by experiments. Min et al. (2005) combined optimally the weighting functions and filters to design a H_2 controller applied to the three-story scaled model with an active mass driver. Abreu et al. (2009) presented a mixed H_2/H_∞ control strategy formulated by means of the LMI approach to attenuate the vibrations of a two-floor building model under seismic excitation.

The main purpose of this paper is to test experimentally the H_2 control technique for optimal control of earthquake excited structures. The control strategy is presented in terms of a general block diagram problem formulation. The controller uses the acceleration signal for feedback. The control design methods are tested on a vibration control experiment consisting of a two-story building test-bed equipped with an active mass driver and subjected to earthquake ground acceleration. A set of experimental tests is made to illustrate the application and delineate the advantages of the control methodology and the performance of the control strategy on the experimental structure is verified.

2. BUILDING STRUCTURAL MODEL WITH ACTIVE MASS DRIVER

A structural dynamic system with an active mass driver (AMD) when subjected to earthquake, as shown in Fig. 1, can be described as

$$\mathbf{M}_{ss}\ddot{x}(t)+\mathbf{C}_{ss}\dot{x}(t)+\mathbf{K}_{ss}x(t)=-\mathbf{M}_{ss}\mathbf{I}\ddot{x}_g(t)+\mathbf{E}_F F(t) \tag{1}$$

where x is the displacement vector of the structure relative to the ground, $\mathbf{M}_{ss}$, $\mathbf{C}_{ss}$ and $\mathbf{K}_{ss}$ are respectively the mass, damping and stiffness matrices of the structure, $\mathbf{I}$ is the identity vector, the subscript g is the acceleration of the ground, $F(t)$ is the control force applied to the structure by the AMD system, and $\mathbf{E}_F$ is the AMD position vector.

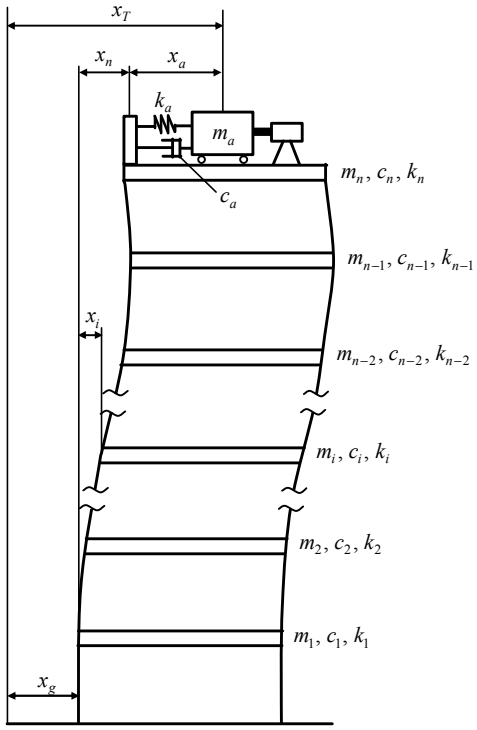

Figure 1. Sketch of building structure with an AMD

The control force $F(t)$ applied to the structure by the AMD can be described as

$$F(t)=k_a x_a(t)+c_a\dot{x}_a(t)-u(t)=m_a\ddot{x}_T(t) \tag{2}$$

where x_a is the displacement of the AMD relative to the top story, m_a, c_a and k_a are the mass, damping and stiffness of the AMD, respectively, $u(t)$ is the force generated by the actuator, and $\ddot{x}_T$ is the absolute acceleration of the AMD, denoted by

$$\ddot{x}_T(t)=\ddot{x}_a+\ddot{x}_n+\ddot{x}_g \tag{3}$$

where $\ddot{x}_n$ is the acceleration of floor where the AMD is installed.

Using the state vector $\mathbf{x}=[x_1 \quad x_2 \quad \cdots \quad x_n \quad x_a \quad \dot{x}_1 \quad \dot{x}_2 \quad \cdots \quad \dot{x}_n \quad \dot{x}_a]$ and combining equations (1) and (2) yields the following state equation

$$\dot{\mathbf{x}}=A_s\mathbf{x}+B_d\ddot{x}_g(t)+B_u u(t) \tag{4}$$

where $A_s=\begin{bmatrix}\mathbf{0} & \mathbf{I}\\ \mathbf{-M_s^{-1}K_s} & \mathbf{-M_s^{-1}C_s}\end{bmatrix}$, $B_d=\begin{bmatrix}\mathbf{0}\\ \mathbf{-E_d}\end{bmatrix}$ and $B_u=\begin{bmatrix}\mathbf{0}\\ \mathbf{M_s^{-1}E_u}\end{bmatrix}$.

The $\mathbf{E_d} = [1 \quad 1 \quad \cdots \quad 1 \quad 0]^T$ and $\mathbf{E_u} = [0 \quad 0 \quad \cdots \quad 0 \quad 1]^T$ are the vector locations relative respectively to the ground and the AMD, and the matrices $\mathbf{M_s}$, $\mathbf{K_s}$ and $\mathbf{C_s}$ are given respectively by

$$\mathbf{M}_s = \begin{bmatrix} m_1 & 0 & 0 & \cdots & 0 \\ 0 & m_2 & 0 & \cdots & 0 \\ \vdots & \vdots & \ddots & \vdots & \vdots \\ 0 & 0 & \cdots & m_n + m_a & m_a \\ 0 & 0 & \cdots & m_a & m_a \end{bmatrix} \tag{5.1}$$

$$\mathbf{K}_s = \begin{bmatrix} k_1 + k_2 & -k_2 & 0 & \cdots & 0 \\ -k_2 & k_2 + k_3 & -k_3 & \cdots & 0 \\ \vdots & \cdots & \ddots & \vdots & \vdots \\ 0 & \cdots & -k_{n-1} & k_n & 0 \\ 0 & \cdots & \cdots & 0 & k_a \end{bmatrix} \tag{5.2}$$

$$\mathbf{C}_s = \begin{bmatrix} c_1 + c_2 & -c_2 & 0 & \cdots & 0 \\ -c_2 & c_2 + c_3 & -c_3 & \cdots & 0 \\ \vdots & \cdots & \ddots & \vdots & \vdots \\ 0 & \cdots & -c_{n-1} & c_n & 0 \\ 0 & \cdots & \cdots & 0 & c_a \end{bmatrix} \tag{5.3}$$

Considering $\mathbf{y} = [\ddot{x}_1 \quad \ddot{x}_2 \quad \ldots \quad \ddot{x}_n \quad x_a]$ as the output of the structural system, that is the absolute acceleration of the floors and the actuator displacement, the vector of measured responses is given by

$$\mathbf{y} = C_y \mathbf{x} + D_{yd} \ddot{x}_g(t) + D_{yu} u(t) \tag{6}$$

where $C_y = \begin{bmatrix} -\mathbf{M_s^{-1}K_s} & -\mathbf{M_s^{-1}C_s} \\ [0 \quad \cdots \quad 0 \quad 1] & [0 \quad 0 \quad \cdots \quad 0] \end{bmatrix}$, $D_{yd} = \begin{bmatrix} -\mathbf{E_d} \\ \mathbf{0} \end{bmatrix}$ and $D_{yu} = \begin{bmatrix} \mathbf{M_s^{-1}E_u} \\ \mathbf{0} \end{bmatrix}$.

3. H_2 OPTIMAL CONTROLLER DESIGN

Consider the general block diagram description of the control problem given in Fig. 2. In this figure, **P** and **K** represent, respectively, the generalized plant and the controller transfer functions, **y** is the output vector of measured structural responses, **z** is the vector of system responses to be controlled, **u** is the control input vector, and **d** is the input vector of excitations representing external disturbances (acceleration ground, wind, etc.) and sensor noise.

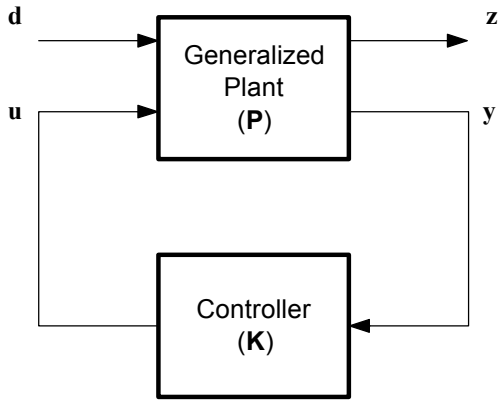

Figure 2. Block Diagram of General Control System with Output Feedback

The generalized plant **P** contains the structural system plus filters and weighting functions in the frequency domain. The regulated output vector **z** may consist of any combination of the states of the system and components of the control

input vector **u**, thus allowing for a broad range of control design objectives to be formulated through appropriate choice of elements of **z**. As depicted in Fig. 3, weighting functions can be applied to the elements of **z** (W_z) to specify the frequency range over which each element of **z** is minimized, W_u weighting the control force vector **u**, and W_g and W_g to shape the spectral content of the disturbance modeling the earthquake excitation and the measurement noise n, respectively. The input excitation vector **d** consists of earthquake excitation $\ddot{x}_g$ and measurement noise n. The output **z** comprises the frequency weighted regulated response (z_r) and control signal. The rectangle denoted with a dashed line in Fig. 3 represents the augmented system model **P**.

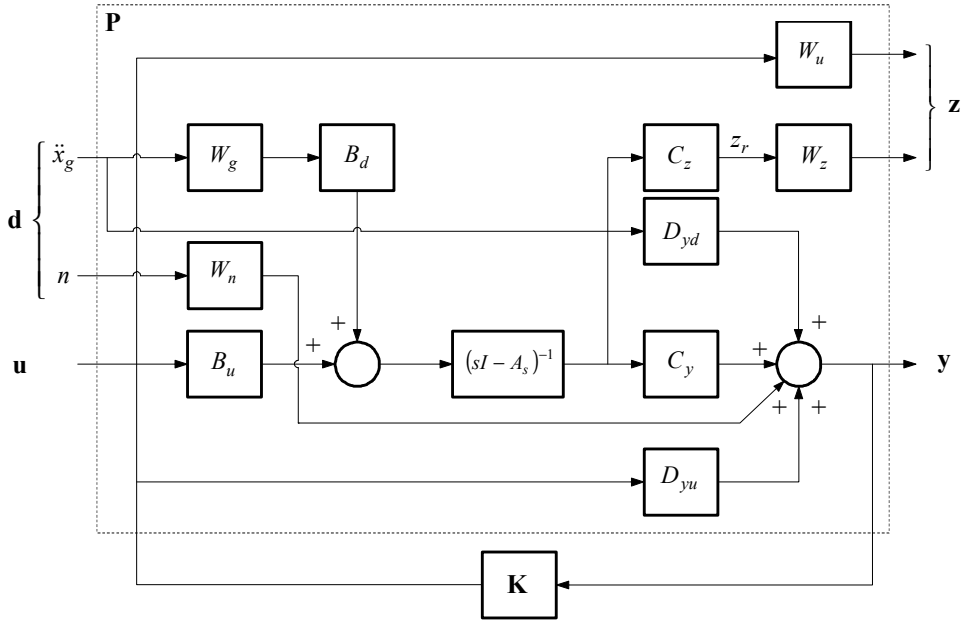

Figure 3. Control block diagram for a building structure subjected to seismic excitation

The regulated response (z_r) denotes the quantities of the design interest that can be floor accelerations, floor displacements or inter-storey drifts, etc. In this work, the outputs to be regulated include the floor displacements and inter-storey drifts

$$z_r = C_z \mathbf{x} = \begin{bmatrix} x_1 & x_2 & \cdots & x_n & x_2 - x_1 & x_3 - x_2 & \cdots & x_n - x_{n-1} \end{bmatrix} \tag{7}$$

where C_z is the appropriate mapping matrix that dictates the components of the regulated response vector z_r.

The block diagram shown in Fig. 3 can be represented in terms of frequency by the equation

$$\begin{bmatrix} \dot{\mathbf{x}} \\ \mathbf{z} \\ \mathbf{y} \end{bmatrix} = \mathbf{P} \begin{bmatrix} \mathbf{x} \\ \mathbf{d} \\ \mathbf{u} \end{bmatrix} \tag{8}$$

where the control vector is **u** = **K** **y** and the state space representation of **P** is given by

$$\mathbf{P} = \left[\begin{array}{c|c|c} A & B_1 & B_2 \\ \hline C_1 & D_{11} & D_{12} \\ \hline C_2 & D_{21} & D_{22} \end{array}\right] = \left[\begin{array}{ccccc|cc|c} A_s & 0 & 0 & C_{W_g} B_d & 0 & 0 & 0 & B_u \\ C_z & A_{W_z} & 0 & 0 & 0 & 0 & 0 & 0 \\ 0 & 0 & A_{W_u} & 0 & 0 & 0 & 0 & B_{W_u} \\ 0 & 0 & 0 & A_{W_g} & 0 & B_{W_g} & 0 & 0 \\ 0 & 0 & 0 & 0 & A_{W_n} & 0 & B_{W_n} & 0 \\ \hline 0 & 0 & C_{W_u} & 0 & 0 & 0 & 0 & D_{W_u} \\ 0 & C_{W_z} & 0 & 0 & 0 & 0 & 0 & 0 \\ \hline C_y & 0 & 0 & C_{W_g} B_d & C_{W_n} & D_{W_g} D_{yd} & D_{W_n} & D_{yu} \end{array}\right] \tag{9}$$

and A_{W_g}, B_{W_g}, C_{W_g}, D_{W_g}; A_{W_n}, B_{W_n}, C_{W_n}, D_{W_n}; A_{W_u}, B_{W_u}, C_{W_u}, D_{W_u}, and A_{W_z} and C_{W_z} are the state space matrices of W_g, W_n, W_u and W_z, respectively.

The task here is to design the controller **K** such that it stabilizes the system and, within the class of all controllers which do so, minimizes the H_2 norm of the transfer function from the disturbances **d** to the regulated output vector **z**. Note that the H_2 norm is given as

$$\|T_{\mathbf{zd}}\|_2 = \sqrt{trace\left\{\frac{1}{2p}\int_{-\infty}^{\infty} T_{\mathbf{zd}}(jw)T_{\mathbf{zd}}^*(jw)dw\right\}} \tag{10}$$

where $j=\sqrt{-1}$ and $T_{\mathbf{zd}}^*$ is the complex conjugate transpose of $T_{\mathbf{zd}}$.

The H_2 control solution procedure in Doyle et al. (1989) is based on the state space realization of the transfer function **P** (Eq. 9) particularly with $\mathbf{D_{11}} = \mathbf{0}$. It can be solved using a standard H_2 control technique assuming (A, B_2) controllable and (C_2, A) detectable. Hence, the full order H_2 controller is expressed by

$$\begin{bmatrix}\dot{\mathbf{x}}_c \\ \mathbf{u}\end{bmatrix} = \mathbf{K}\begin{bmatrix}\mathbf{x}_c \\ \mathbf{y}\end{bmatrix}; \qquad \mathbf{K} = \left[\begin{array}{c|c} A_k & B_k \\ \hline C_k & 0 \end{array}\right] \tag{11}$$

where

$$A_k = A + K_f C_2 + B_2 K_c + K_f D_{22} K_c \tag{12.1}$$

$$B_k = -K_f \tag{12.2}$$

$$C_k = K_c \tag{12.3}$$

where

$$K_f = -YC_2^T - B_1 D_{21}^T \tag{13.1}$$

and

$$K_c = -B_2^T X - D_{12}^T C_1 \tag{13.2}$$

The matrices and X and Y are solutions to the corresponding algebraic Riccati equations

$$\left(A - B_2 D_{12}^T C_1\right)^T X + X\left(A - B_2 D_{12}^T C_1\right) - XB_2 B_2^T X + C_1^T C_1 = 0 \tag{14.1}$$

$$Y\left(A^T - C_2^T D_{21} B_1^T\right)^T + \left(A^T - C_2^T D_{21} B_1^T\right)Y - YC_2^T C_2 Y + B_1 B_1^T = 0 \tag{14.2}$$

4. EXPERIMENTAL EXAMPLE

In this section, an experimental example is presented to illustrate the usefulness of the control method presented in previous section. Consider the linear system consisting of a building model (see Fig. 4a), manufactured by Quanser Consulting Inc, with two floors, equipped with AMD and subjected to earthquake ground acceleration ($\ddot{x}_g$) using the shake-table system. The test structure has 1125 mm in height, with each column being steel with a section of 1.75 × 108 mm. The total mass of the structure is 4.52 kg, where the first floor mass (m_1) is 1.16 kg, the second floor mass (m_2) is 1.38 kg.

As shown in Fig. 4, the structure is fully instrumented to provide for a complete record of the motions undergone by the structure during testing. Each floor of the building structure is equipped witch a capacitive DC accelerometer that measures the absolute accelerations ($\ddot{x}_1$ and $\ddot{x}_2$). The accelerometers are manufactured by Quanser Consulting Inc., and produce an output of ± 5 V with a range of ± 5 g. Two universal power modules are used as power amplifiers; one of them is used to power the shaking table and the other one is used to power the AMD. The data acquisition and control board used to collect data and drive the power amplifier is a MultiQ-PCI. Features of the board include an 8-channel analog-to-digital converter with an input range of ± 10 V, 14-bit resolution. In addition, the board contains an 8-channel digital-to-analog converter with an output range of ± 10 V and 12-bit resolution.

A diagram of the control system is shown in Fig. 4b. The structure is controlled by the AMD, subjected to shaking table movement excitation. The acceleration signals on both stories and the displacement of the AMD are used as feedback signals after amplification and passage through the A/D converter. Using the proposed controller, a control signal is produced (v_m) based on the feedback signals. After passage through the D/A converter and amplification, the control signal is sent to the AMD device and it generates a control force (u). Digital control is achieved by use of the MultiQ-PCI board with the *QuaRC* realtime controller. The controller is developed using *Matlab Simulink*® and executed in realtime using the *QuaRC* software. The *Simulink* code is automatically converted to *C* code and interfaced through the *QuaRC* software to run the control algorithm.

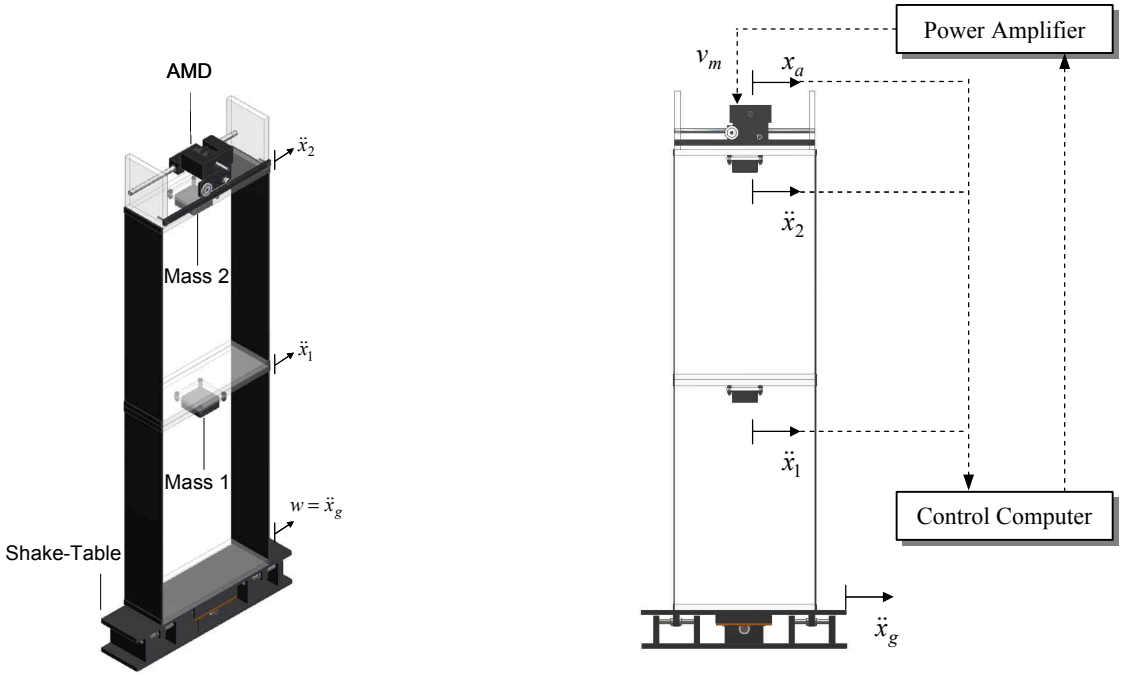

Figure 4. Two-floor building model (a) and schematic of experimental setup (b)

The AMD consists of a moving cart with a DC motor that drives the cart along a geared rack through the motor pinion. Additionally, a potentiometer is attached to the motor to measure the cart position relative (x_a) to its base. The maximum stroke is ± 65 mm and the total moving mass is 520 g (m_a). The AMD provides the control force (u) to the structure through the control voltage (v_m) (Quanser Consulting Corporation, 2003)

$$u(t) = \frac{k_g k_m}{R_a r_p} v_m(t) - \frac{k_g^2 k_m k_{cem}}{R_a r_p^2} \dot{x}_a(t) \tag{15}$$

where k_g is the gear-box ratio, r_p is the pinion radius, R_a is the motor armature resistance, and k_m and k_{cem} are respectively the cart motor torque and cart back-electromotive force constants.

Table 1 lists and characterizes the main parameters (mechanical and electrical specifications) associated with the structural system equipped with AMD.

Table 1. Main parameters associated with the structural system.

Parameter	Symbol	Value
First Floor Mass	m_1	1.16 *Kg*
Second Floor Mass	m_2	1.38 *Kg*
Cart Mass	m_a	0.52 *Kg*
First and Second Floors Linear Stiffness	k_1, k_2	500 *N/m*
First and Second Floors Damping Coefficients	c_1, c_2	10^{-3} *N.s/m*
Gear-box Ratio	k_g	3.71
Cart Motor Torque Constant	k_m	0.00767 *N.m/A*
Cart Back-ElectroMotive Force Constant	k_{cem}	0.00767 *V.s/rad*
Cart Motor Armature Resistance	R_a	2.6 Ω
Cart Motor Pinion Radius	r_p	6.35 *mm*

It should be noted from Eq. (15) that the damping coefficient of the cart is $c_a = \frac{k_g^2 k_m k_{cem}}{R_a r_p^2}$ and the Coulomb friction (nonlinear) applied to the linear cart has been neglected. Furthermore, the stiffness associated to the cart (k_a) has also been neglected.

4.1. Controller Design

The choice of weighting functions is crucial for obtaining meaningful controller performance results. In general, a direct application of the H_2 optimization seeks to minimizing the H_2 norm over all frequencies without placing more emphasis or penalty on certain frequency ranges. For the control model used in this study, frequency-dependent weighting function W_g is employed to reflect the frequency content of an earthquake. The most commonly used stochastic model of earthquakes is the square root of the Kanai-Tajimi spectrum (Spencer et al., 1994)

$$W_g(s) = \frac{\sqrt{S_0}\left(2z_g w_g s + w_g^2\right)}{s^2 + 2z_g w_g s + w_g^2} \tag{16}$$

where the parameters of the Kanai-Tajimi spectrum used in this paper are $S_0 = 0.005$, $z_g = 0.5$, and $w_g = 15$ rad/s.

The frequency responses of W_g and of the ground excitation chosen for this study (scaled El Centro earthquake) are shown in Fig. 5.

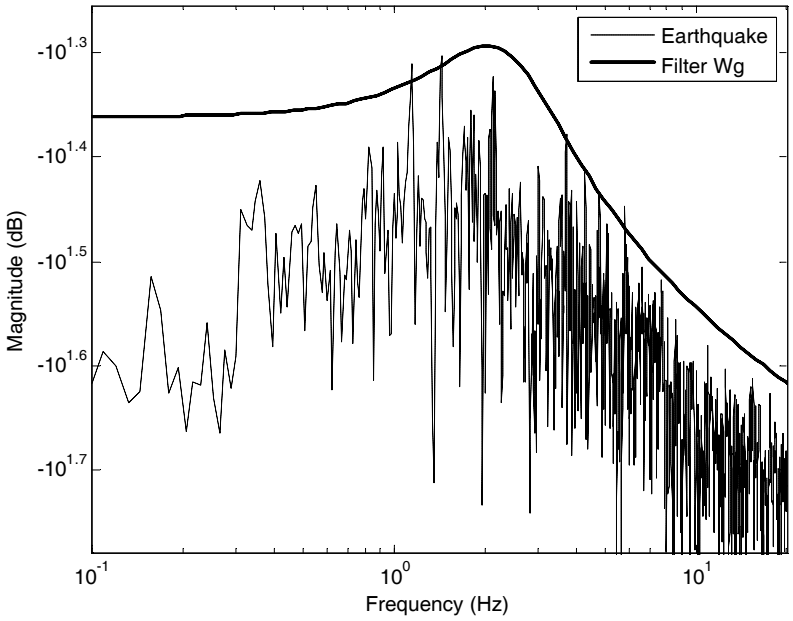

Figure 5. Frequency responses of the Scaled El Centro earthquake and filter W_g

In this paper, for the regulated output responses z and the measurement noise n in Fig. 3, the weighting functions W_z, W_u and W_n are respectively selected as

$$W_z = 100 \times \mathbf{I}_{3\times 3} \tag{17.1}$$

$$W_u = 0.2 \tag{17.2}$$

$$W_n = 0.1 \times \mathbf{I}_{3\times 3} \tag{17.3}$$

which means that the regulated output responses z_r, the control signal u (0.2 corresponds to a maximum of 5 Volts) and the measurement noise (0.1 is estimate of the sensor noise levels) are weighted in the entire frequency region.

4.2. Experimental Results

To demonstrate the performance of the designed H_2 optimal controller, shaking table test of the two-story building model with AMD introduced previously was conducted. An earthquake-type excitation was inputted to the shake-table system as the excitation source. The building test-bed on the shaking table was excited by the scaled El Centro earthquake signal shown in Fig. 6.

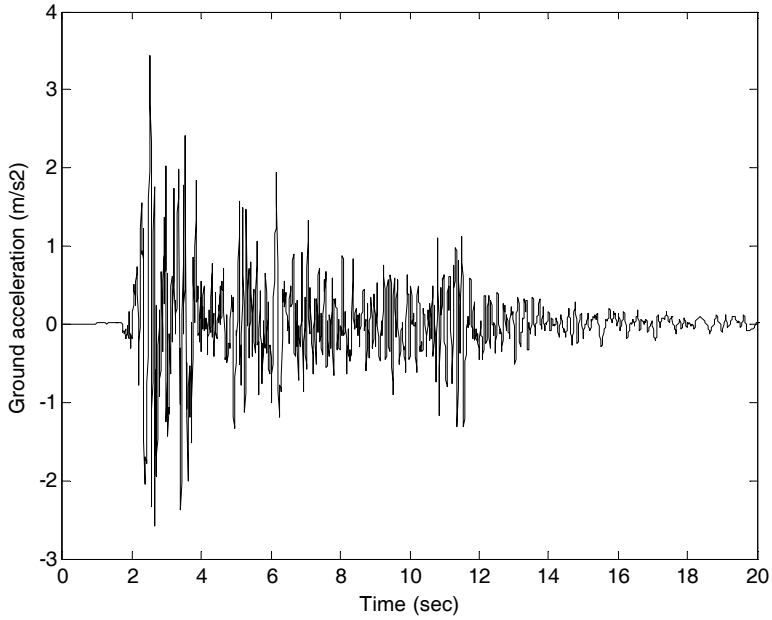

Figure 6. El Centro earthquake ground acceleration used for seismic excitation

The controller is implemented using the Matlab Simulink® interface and executed in realtime using the QuaRC software. A schematic diagram of the control system is presented in Fig. 1. Figure 7 illustrates the block diagram developed for the seismic response control system. A proportional-derivative (PD) controller is used for shake-table position control using the position reference shown in Fig. 8.

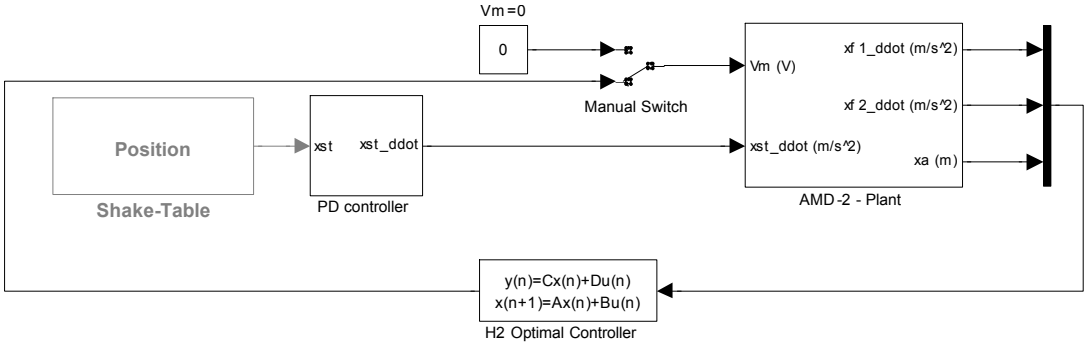

Figure 7. Simulink® block diagram for a seismic response control system

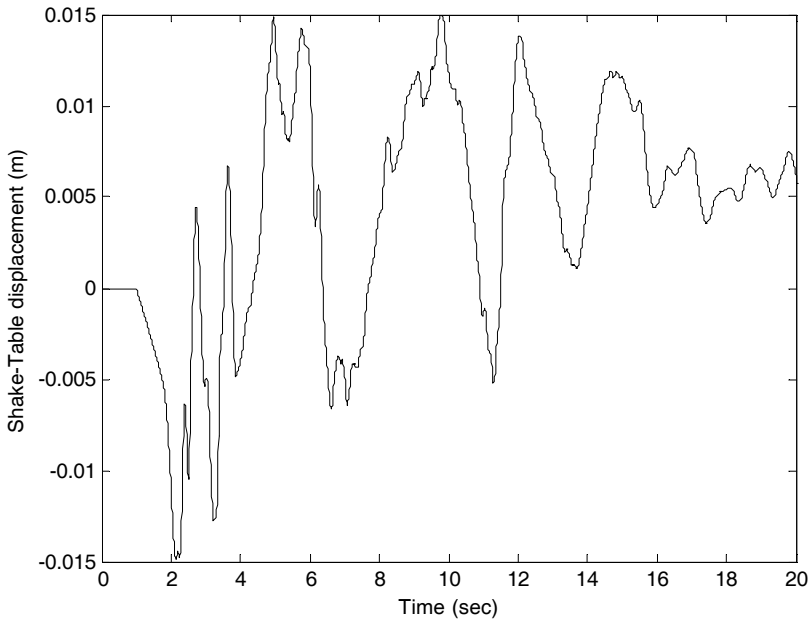

Figure 8. Shake-Table position reference used by the PD controller.

Figure 9 shows the acceleration of the first floor ($\ddot{x}_1$) and the second floor ($\ddot{x}_2$) of the bench-scale structure when excited by the scaled El Centro earthquake signal for the controlled and uncontrolled systems. From the results it can be observed that the structural responses are reduced greatly. The reduction ratios of the acceleration in the first floor and second floor are 88% and 69%, respectively.

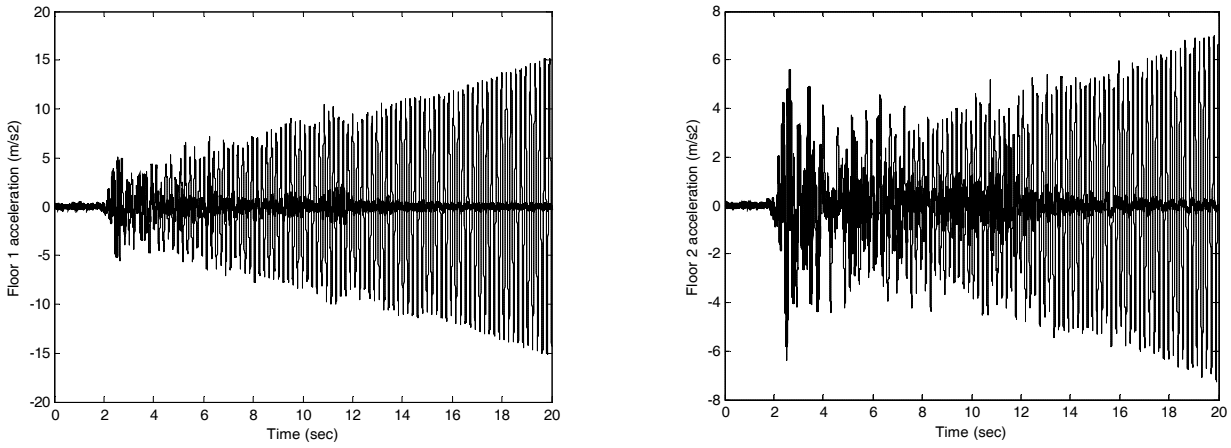

(a) (b)

Figure 9. Open (dashed) and closed loop (solid) acceleration responses of floors 1 (a) and 2 (b) under seismic excitation

The AMD input voltage (v_m) and its associated position (x_a) are illustrated in Fig. 10. As can be seen from Fig. 10 (b), note that the AMD do not reach its stroke limit (± 65 mm), i.e., the actuator saturation.

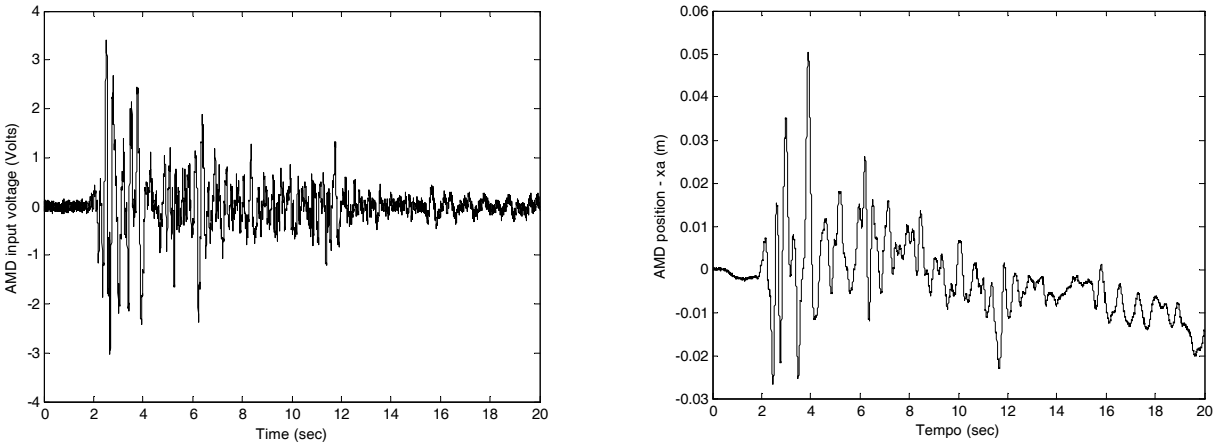

(a) (b)

Figure 10. AMD input voltage v_m (a) and its associated position x_a (b)

5. CONCLUSIONS

The optimal H_2 control strategy was tested to attenuate the vibrations of a two-floor building model under seismic excitation. The goal of this approach is to design an output feedback H_2 controller which minimizes the disturbance attenuation level considering the control input limit and the shape of the disturbance excitation. It is shown that when the optimal H_2 control strategy is used in the bench-scale structure, the experimental results show that the structural responses are reduced significantly with the designed optimal controller. The inclusion of uncertainties in the controller design constitutes the next implementation for this research.

6. ACKNOWLEDGEMENTS

The first author would like to thank the FAPESP (Nº 2008/05129-3) for the financial support of the reported research.

7. REFERENCES

Abreu, G. L. C. M., Lopes Jr., V. and Brennan, M. J., 2009, "Mixed H_2/H_∞ Control of a Two-Floors Building Model using the Linear Matrix Inequality Approach", 20th International Congress of Mechanical Engineering – COBEM2009, Gramado-RS, Brasil.

Doyle, J.C., Glover K., Khargonekar, P. and Francis, B., 1989, "State-Space Solutions to Standard H_2 and H_∞ Control Problems", IEEE Transactions on Automatic Control, Vol. 34, No. 8, pp. 831-847.

Dyke, S. J., Spencer, B. F., Quast, P., Kaspari, D. C. and Sain, M. K., 1996, "Implementation of an Active Mass Driver using Acceleration Feedback Control", Microcomputers in Civil Engineering, Vol. 11, pp. 305-323.

Housner, G. W., Bergman, L. A., Caughey, T. K., Chassiakos, A. G., Claus, R. O., Masri, S F., Skelton, R. E., Spencer, B. F. and Yao, J. T., 1997, "Structural Control: Past, Present and Future", Journal of Engineering Mechanics, ASCE, Vol. 9, pp. 897-971.

Min, K. W., Joo, S. J. and Kim, J., 2005, "Design of Frequency Dependent Weighting Functions for H_2 Control of Seismic Excited Structures", Vol. 11, pp. 137-157.

Quanser Consulting Corporation, 2003, "Active Mass Damper – Two Floors: User Manual", Ontario, Canada.

Spencer, B. F., Suhardjo, J. and Sain, M. K., 1994, "Frequency Domain Optimal Control Strategies for a Seismic Protection", Journal of Engineering Mechanics, Vol. 120, pp. 135-159.

Spencer, B. F. and Sain, M. K., 1997, "Controlling Buildings: A New Frontier in Feedback", IEEE Control System Magazine on Emerging Technology, Vol. 17, No. 6, pp. 19-35.

Suhardjo, J., Spencer, B. F. and Kareem, A., 1992, "Frequency Domain Optimal Control of Wind Excited Buildings", Journal of Engineering Mechanics, ASCE, Vol. 118, No. 12, pp. 2463-2481.

8. RESPONSIBILITY NOTICE

The authors are the only responsible for the printed material included in this paper.